Available online at www.sciencedirect.com
SciVerse ScienceDirect
Ceramics International 38 (2012) 5445–5451
CERAMICS INTERNATIONAL
www.elsevier.com/locate/ceramint

Antibacterial activity of silver photodeposited nepheline thin film coatings

Ali Ghafari-Nazari [a,b,*], Fathollah Moztarzadeh [c], Sayed Mahmood Rabiee [d], Talieh Rajabloo [b], Masoud Mozafari [c,e,**], Lobat Tayebi [e]

[a] Department of Mechanical and Industrial Engineering, University of Brescia, Via Branze 38, 25123 Brescia, Italy
[b] Materials Engineering Department, Islamic Azad University, Southern Branch, Tehran, Iran
[c] Biomaterials Group, Faculty of Biomedical Engineering (Center of Excellence), Amirkabir University of Technology, P.O. Box 15875-4413, Tehran, Iran
[d] Mechanical Engineering Department, Babol University of Technology, Babol, Mazandaran, Iran
[e] Helmerich Advanced Technology Research Center, School of Material Science and Engineering, Oklahoma State University, OK 74106, USA

Received 5 March 2012; received in revised form 18 March 2012; accepted 23 March 2012
Available online 31 March 2012

Abstract

Antibacterial characteristic of silver makes this material very appealing for surface coating on various substrates. In this study, we investigated different silver containing powder for this purpose. Specifically we examined the antibacterial activity of Ag/nepheline compared with Ag/TiO_2 and Ag/SiO_2. Our analysis suggested ‘‘Ag/nepheline’’ composite thin film is an appropriate coating for production of antibacterial ceramic tiles in large scale. In our investigation, FactSage software was used for the thermodynamic analysis. Nano-silver was obtained from silver nitrate solution by ultraviolet illumination of distilled water. In this process, silver was doped on micronized TiO_2, SiO_2, or nepheline. The silver composites and monolithic silver were sprayed with water on raw tiles and sintered in a furnace. Exploring the results suggested the best component for achieving antibacterial tile is Ag/nepheline.

Keywords: B. Surfaces; Photodeposition; Nepheline; Silver; Antibacteria; Coating

1. Introduction

The strong antimicrobial activity of silver nanoparticles is the major direction for the recent development of this material with diverse applications. They are being used in different products such as room spays, laundry detergents, water purifications, glasses, tiles, and wall paints [1–4]. In medical supplies, there are wound dressings, contraceptive devices, surgical instruments and bone prostheses coated or embedded with silver nanoparticles [5–8]. They are also incorporated into textiles for manufacturing clothing, underwear, socks [9,10]. The processing of silver nanoparticles or composites can be classified into several methods such as chemical reduction [11], reversed micelle [12], sol–gel [13], ultrasonic radiation [14], biochemical [11], hydrothermal [15], microwave irradiation [16] and photocatalytic reduction [17,18]. In all above methods, nano-sized silver particles can be synthesized only with a low concentration of silver colloids (several millimoles per liter or less).

Common component for antibacterial composites is TiO_2 [19–22] which is an opaque agent of glaze [23]. Thus, it is not an appropriate element in types of glazes where transparency is important. SiO_2 is the basement of glaze structure [23]. The antibacterial activity of Ag/SiO_2 had been investigated previously [13,24,25].

Nepheline is a glaze flux material stronger than feldspars [23]. With our best knowledge, the antibacterial activity of Ag/nepheline thin films has not yet been investigated and is the subject of this manuscript. Nepheline is an igneous rock. Its coarse-grained appearance is similar to granite with lower proportion of silica. Nepheline is a feldspathoid mineral of composition (Na, K) $AlSiO_4$ and usually forms small grains, which are intercrystallized with the feldspar.

* Corresponding author at: Department of Mechanical and Industrial Engineering, University of Brescia, Via Branze 38, 25123 Brescia, Italy. Tel.: +39 0303715574.
** Co-corresponding author at: Helmerich Advanced Technology Research Center, School of Material Science and Engineering, Oklahoma State University, OK 74106, USA. Tel.: +1 918 594 8634; fax: +1 270 897 1179.
E-mail addresses: ali.ghafari@ing.unibs.it (A. Ghafari-Nazari), masoud.mozafari@okstate.edu (M. Mozafari).

0272-8842/$36.00 © 2012 Elsevier Ltd and Techna Group S.r.l. All rights reserved.
http://dx.doi.org/10.1016/j.ceramint.2012.03.055

Compared to pure feldspars, the ratio of potassium and sodium in composition of nepheline is larger. $K_2O + Na_2O$ is about 9–12 wt% in feldspars but more than 14 wt%, in nepheline. The melting temperature of nepheline is lower than that of potassium-feldspar [26]. According to Burat et al. [27] nepheline has higher ratio of alkali/alumina than feldspar. Therefore less amount of it is required to achieve a comparable fluxing action. Hence, nepheline is often preferred in container glass batches as raw material handling, storage and energy is more economical [27,28].

In this research, we investigated the silver solution ($AgNO_3 \rightarrow Ag^+$) and precipitation ($Ag^+ \rightarrow Ag_{(s)}$) conditions by FactSage software [29]. Using the optimum condition for precipitation of silver on nepheline, we studied the antibacterial activity of Ag–nepheline compared with that of Ag–TiO_2 and Ag–SiO_2 thin films.

2. Experimental procedures

2.1. Construction of photocatalytic reaction container

A photocatalytic reaction container is made from stainless steel (316) with three 250 W Ultra Violet (UV) lamps installed on its top. The size of the container was 80 cm in diameter and 60 cm in height. A controllable spinning motor was also designed to make a homogenous solution.

2.2. Preparation of silver-containing thin films

Silver nitrate ($AgNO_3$, 99%) and poly vinyl pyrrolidone (PVP, 98%) were purchased form Aldrich and Merck respectively. Also, TiO_2, SiO_2 and nepheline (<95 wt% purity) from industrial clays of Iranian mining were utilized. Distilled water, $AgNO_3$ and PVP (5 wt%) were carefully mixed in a container. The amount of silver in composite films was set at 5 wt% according to previous reports [24,30–32]. After 2 h of mixing, TiO_2, SiO_2 or nepheline was added to the mixture. Also, a monolithic silver thin film was synthesized without addition of these components. Finally, UV lamps were illuminated.

The experiments were done at room condition. At the end of the synthesis process, the color of solution was stable [33]. The mixture of this solution and water (weight ratio of 1:10) were sprayed on the ceramic tiles by a spray gun. The coated tiles as well as conventional tiles were sintered.

2.3. Antibacterial tests

The antibacterial behaviors of tiles were evaluated against two bacterial strains: gram-negative *Escherichia coli* and Gram-positive *Staphylococcus aureus* using 1/2McFarland method. In order to study the antibacterial activity of the tiles, *E. coli* and *S. aureus* were deposited on the coated one tile slides (5 cm × 5 cm). We used uncoated tile slides as a control. Each slide was placed in a sterile vial and the tiles were subjected to a pretreatment with 800 μl distilled water for 10 min. Tryptone soy broth (2.2 ml) was then added to each vial to have total volume of 3 ml. An aliquot (10 μl) of *S. aureus* or *E. coli* suspension was added to each vial (1.6×10^3 ml^{-1}) containing the slides. Control broths with and without bacterial inoculation were also included. The vials were incubated with agitation at 35 °C, 220 rpm. Aliquots of 10 μl broth were sampled at 24 h and serial dilutions for the aliquots were prepared in broth. Duplicate aliquots (50 μl) of the serially diluted samples were spread on the plates. The plates were incubated at 35 °C and bacterial counts were performed. The bacteriostatic activity was evaluated after 24 h and the percentage of bacteria reduction was calculated using the following equation (1):

$$R(\%) = \frac{A - B}{A} \times 100 \quad (1)$$

In which R is the reduction rate, A is the number of bacterial colonies from untreated tiles and B is the number of bacterial colonies from the treated tiles [34]. In contrast, in order to evaluate the antimicrobial behavior of composites, the procedure was kept the same for tiles, but the sizes of inhibitory circle for the antibacterial disks were measured [35]. For these samples, the bacteriostatic activity was calculated using Eq. (1), where A is the radius from composites and B is the radius from control samples.

2.4. Characterization

To perform the electron microscopy imaging, samples were coated with a thin layer of gold (Au) by sputtering (EMITECH K450X, England) to promote electrical conductivity. Morphology and microstructure of samples were observed using SEM (Seron Technology, model AIS-2100) at an acceleration voltage of 30 kV.

Firing behavior was appraised by determining fusibility of clay materials by hot-stage microscopy (Expert System Misura, 10 °C min^{-1} up to 1600 °C) inferring the characteristic temperatures T_{sint} (beginning of densification), T_{soft} (softening), $T_{1/2sphe}$ (half of sphere), T_{sphe} (sphere), and T_{fusi} (fusion) through morphological changes occurring to a cylindrical specimen (3 mm height and 2 mm diameter) with an uncertainty of 5–10 °C [36].

3. Results and discussion

3.1. Thermodynamic of silver precipitation

The thermodynamic of silver precipitation was simulated at the presence of silver nitrate and water (other raw materials do not have any effect on this system).

At the state of solution ($AgNO_3 \rightarrow Ag^+$), E–pH diagrams calculated by FactSage software. We investigated condition of solution for obtaining more silver ion instead of other silver components. According to the results from FactSage software, by increasing the silver nitrate (from 10^{-4} to 10 mol), the stable area of silver ion (from pH = 10.2 to pH = 5.2) and silver hydroxide decreased (Fig. 1). Therefore, the amount of silver nitrate in water must decrease for getting a more stable silver ion from silver nitrate.

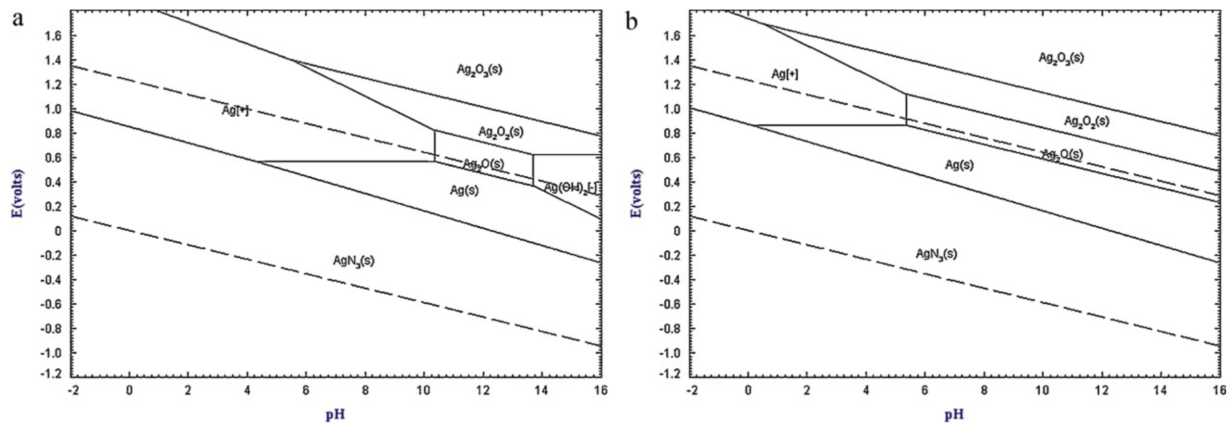

Fig. 1. E–pH diagram for (a) 10^{-4} and (b) 10 mol $AgNO_3$ in water.

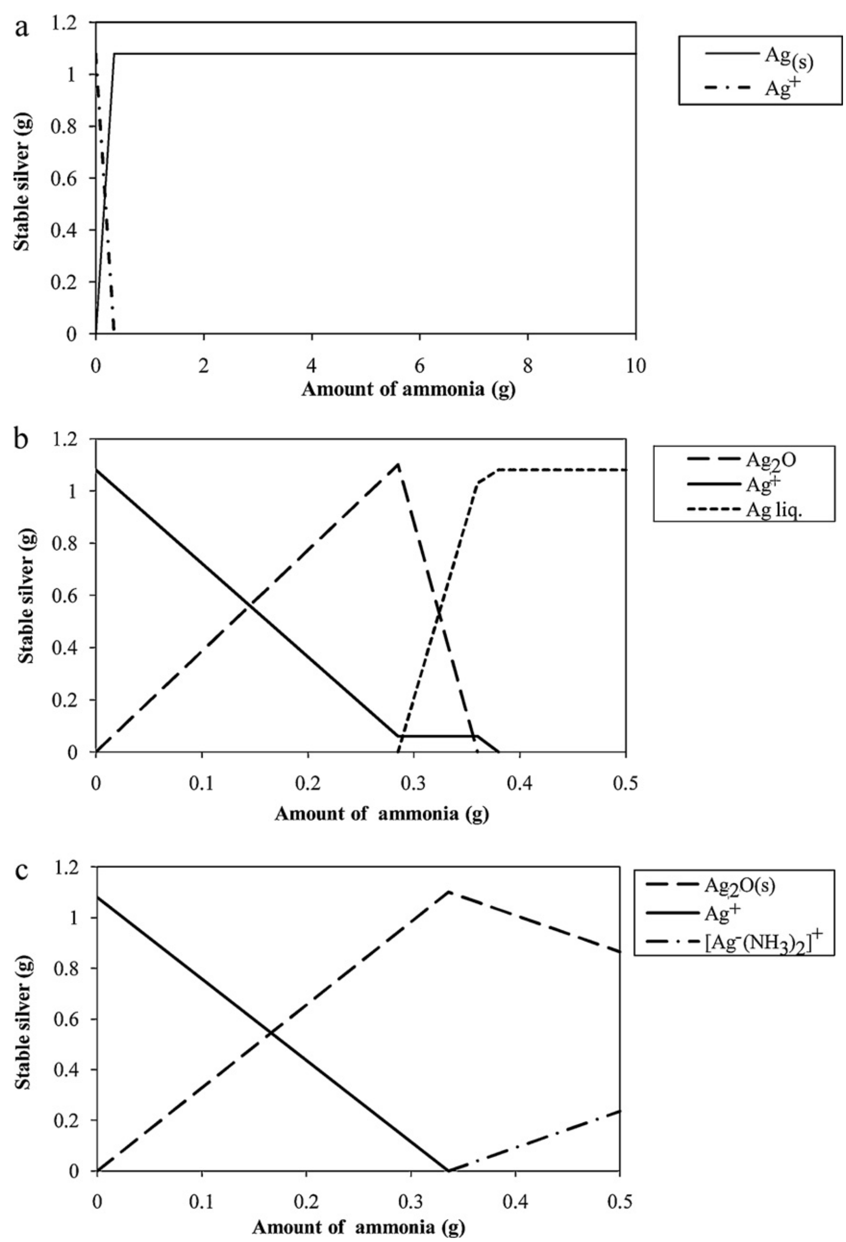

Fig. 2. (a) Stable condition of silver nitrate solution during increasing the amount of ammonia. (b) Removing silver solid from database of software. (c) Removing of silver solid and liquid from database of software.

According to Eq. (2), silver nitrate in water, at thermodynamic standard state, was completely ionized with reaction conditions of $\Delta H = -1.58761$ J, $\Delta G = -1.70421 \times 10^6$ J and pH = 6.985.

$$1.7\ \text{g}\ AgNO_3 + 100\ \text{g}\ H_2O \rightarrow 1.08\ \text{g}\ Ag^+ + 0.62\,\text{g}\ NO_3{}^- + 100\ \text{g}\ H_2O \quad (2)$$

In some studies [22,37,38], use of ammonia was suggested to obtain a better precipitation. It is claimed that by addition of ammonia to aqueous solution of $AgNO_3$, a complex of silver may form (i.e., $[Ag^-(NH_3)_2]^+$). By this complex, the precipitation of silver can be occurred faster under the ambient light.

The stable conditions of reaction (2) with NH_3 ($0 \le x \le 10$ with 0.001 g step) were investigated. The results summarized in Fig. 2(a). It is indicated that by further addition of ammonia to 0.343 g, the amount of silver ion decreased and silver solid precipitated. It is important to point out Zhang et al. [11] also showed the addition of nitro compounds led to the synthesis of pure silver particles. It is possible that other components of silver instead of solid silver synthesized due to kinetic barriers. So it is reasonable to solve this condition by investigating the reaction system by omitting solid silver from the database of software. According to Fig. 2(b), by consuming the silver ion, the silver oxide was precipitated. Note that when this reaction was completely done, the liquid silver began nucleation. Finally, by removing the liquid silver from the database and after supersaturation of silver oxide $[Ag^-(NH_3)_2]^+$ complex obtained as shown in Fig. 2(c). These findings are in accordance with previous studied. According to Zhang et al. [22] the formation of silver liquid was unbelievable at this condition.

It can be concluded that the agent of rapid precipitation in the work of Zhang et al. [22] was silver oxide as the initiator of nucleation with a very low antibacterial activity [31]. Thus, when antibacterial surfaces are desired, this method is not appropriate. Applying the ammonia leads to the formation of a small amount of silver complex after supersaturation of silver oxide in the reaction system. Another disadvantage of this idea is the excessive use of ammonia which results in the destruction of surface [23].

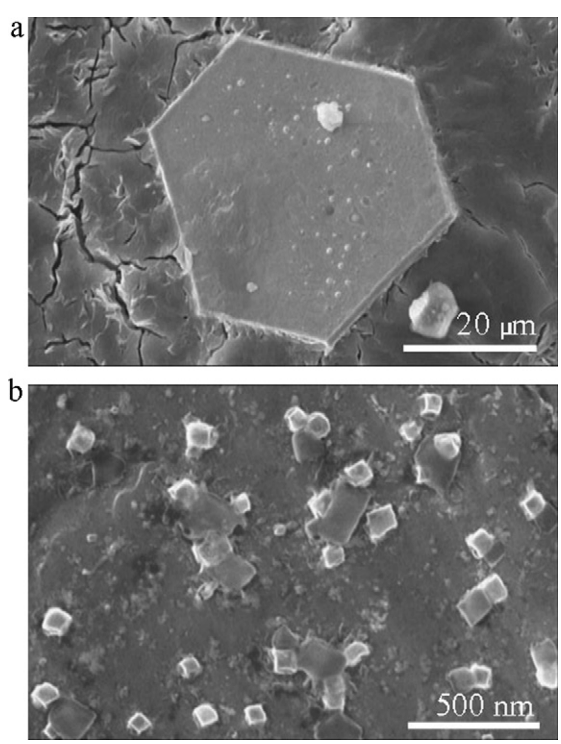

Fig. 3. SEM of monolithic silver from (a) 2 wt% $AgNO_3$ and (b) 0.5 wt% $AgNO_3$ in water.

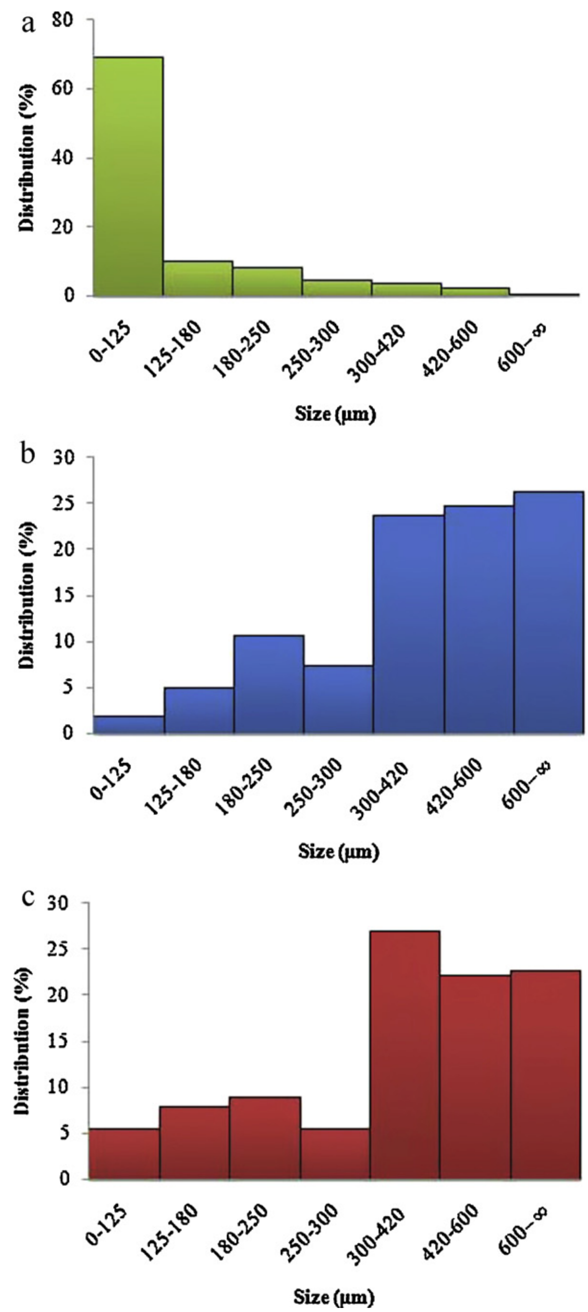

Fig. 4. Size distribution of composites substrates by conventional screening for (a) nepheline, (b) SiO_2, and (c) TiO_2.

3.2. Monolithic silver

Monolithic silver particles were synthesized by mixing $AgNO_3$ (2 wt%), PVP and distilled water. After illumination, the solution became a little dark. This reaction was done after 9.5 h. Fig. 3(a) shows a well-defined hexagonal plate of silver. The bacteriostatic activity was stable after 3 months.

To investigate the effect of materials concentration during the synthesis process the amount of $AgNO_3$ decreased to 0.5 wt%. Surprisingly, as it can be seen in Fig. 3(b), nano-sized silver particles achieved in cubic morphology. The reaction time was the same, but the bacteriostatic activity was four times higher. Knauth et al. [39], and Suber et al. [40] also showed that by changing the conditions, the size and morphology of silver particles became completely different. It is obvious that the cubic homogenous silver particles nucleated by making suitable conditions. By increasing the silver ions in the reaction system, nucleation grew in the shape of hexagonal plates. It suggested that the growth direction in A axial is equal to B axial, but C axial is lower than them.

3.3. Silver composites

3.3.1. Comparison of oxides

Size distribution of TiO_2, SiO_2 and nepheline particles is shown in Fig. 4 obtained by conventional screening method. The size distribution of TiO_2 and SiO_2 is in the range of 125–600 μm. However, nepheline is finer than the others. About 70 wt% of nepheline particles are smaller than 125 μm. Another benefit of nepheline is the lowest amount of iron component. TiO_2, SiO_2 and nepheline have 1.02, 2.54 and 0.09 wt% iron oxides respectively. Iron oxides form black points in the surface of glaze [23], which have a bad effect on the thermal, chemical and mechanical resistance of tiles.

3.3.2. Ag/TiO_2 composite

In the first step, 5 wt% Ag/TiO_2 composite was obtained by using 0.2 wt% $AgNO_3$, PVP and 2.5 wt% TiO_2, and UV illumination, as shown in Fig. 5(a). This reaction was completed after 8.5 h because the TiO_2 particles act as nucleation agent that led to decrease of reaction time. The visual appearance of the composite was inhomogenous (white and brown) due to the precipitation of output at the bottom during illumination. The problem was resolved by using kaolin powder which is a kind of alumina-silicate component [23]. Due to the low amount of zeta potential, it leads to the suspension of composites in water for a long time.

3.3.3. Synthesis of Ag/SiO_2 composite

For obtaining 5 wt% Ag/SiO_2 composite, 0.2 wt% $AgNO_3$, PVP and 2.5 wt% SiO_2 were mixed and then UV was illuminated as shown in Fig. 5(b). This reaction was not completed after 16 h and the problem of precipitation was higher than TiO_2 (low speed of reaction and precipitation). Also, spraying silica on the surface of tiles led to the creation of black points on the tiles due to the existence of the large amount of iron components. We did not find a solution for this problem.

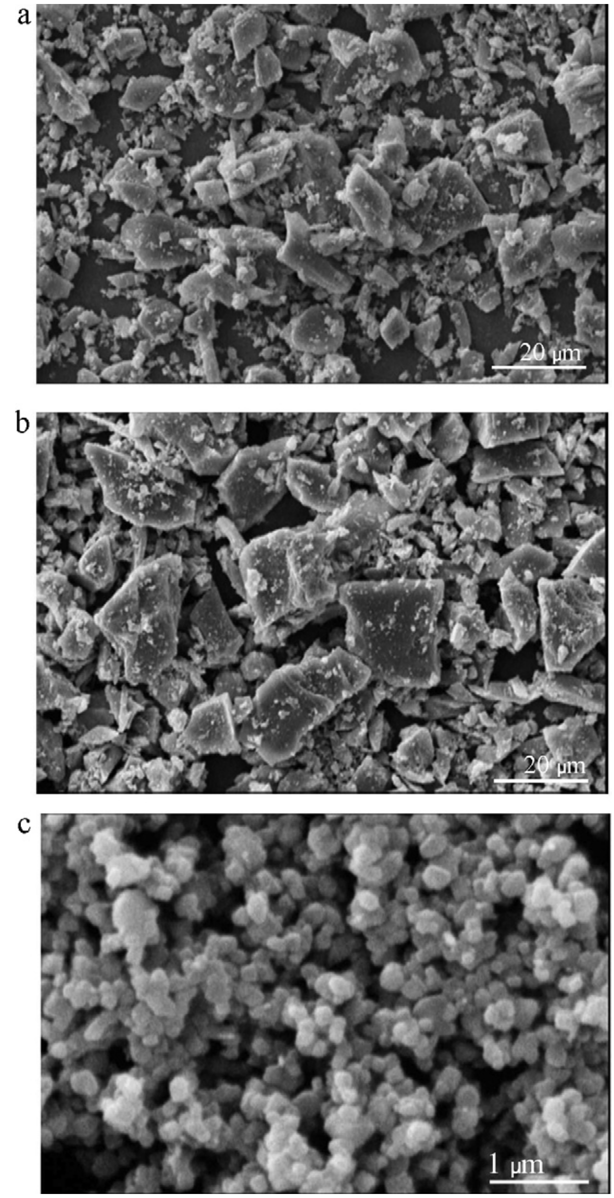

Fig. 5. SEM micrograph of (a) 5 wt% Ag/TiO_2, (b) 5 wt% Ag/SiO_2, and (c) 5 wt% Ag/nepheline composite in water.

3.3.4. Synthesis of Ag/nepheline composite

For acquiring 5 wt% Ag/nepheline composite, 0.2 wt% $AgNO_3$, PVP and 2.5 wt% nepheline were mixed and then UV was illuminated. This reaction was completed after 4 h without significant precipitation which led to homogenous slurry. Fig. 5(c) shows the morphology of Ag/nepheline composite. Shape and size of nepheline feature is very different. Based on Figs. 4 and 5, the size distribution of SiO_2 is similar to TiO_2, but nepheline is very finer. This advantage of nepheline led to a good distribution in the container without precipitation. Another benefit of smaller size was the production of antibacterial tile which can be distributed on the glaze in a good manner. Owing to the fact that nepheline had finer particles; the rate of nucleation was higher than that of other oxides. By increasing the rate of nucleation, silver particles

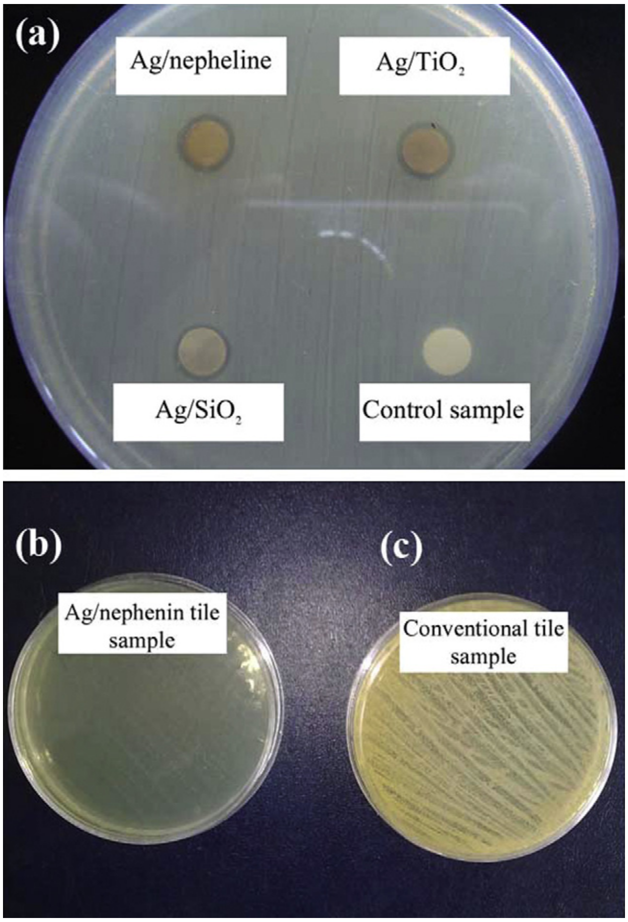

Fig. 6. (a) Photograph of the inhibitory circle for antibacterial disks of silver composites against *S. aureus* (the control sample is water). (b) The bacteriostatic activity of tile coated with Ag/nepheline composite, (c) conventional tile sample.

were finer [38], and the bacteriostatic activity was higher [31]. These convolutions were in agreement with the experiments.

3.4. Antibacterial activity

Among these three oxides, the antibacterial activity of nepheline was stronger. The bacteriostatic activity of nepheline was 85% against *E. coli* and 80% against *S. aureus*. However, this rate for TiO_2 was 62% and 48% against *E. coli* and *S. aureus* respectively. The bacteriostatic activity of SiO_2 has the lowest rate among these three: 30% against *E. coli* and 26% against *S. aureus*. In these calculations, the control was the same solution without silver. An image of inhibitory circle against *S. aureus* is shown in Fig. 6(a). Also, the effect of the bacteriostatic activity after spraying and sintering composites on the tiles is shown in Fig. 6(b) and (c). It can be seen that the antibacterial activity of Ag/nepheline composite (around 99.9%) is higher than other composites. Also, the bacteriostatic activities of monolithic silver and SiO_2 samples were less than 5%.

If the humidity of the tile increases, the tile will shatter in the furnace. After UV illumination of silver on nepheline, the ratio of solution to water in the spray gun decreased from 1:10 to 1:5. The effect of spraying in the bacteriostatic activity of Ag/nepheline is shown in Fig. 7. Note that Fig. 6(a) is associated to a tile after one time spraying of Ag/nepheline. It is worth mentioning that the bacteriostatic activity of Ag/nepheline sample was higher than the other kinds of silver-containing composites due to more antibacterial activity and best compatibility with surface of tiles.

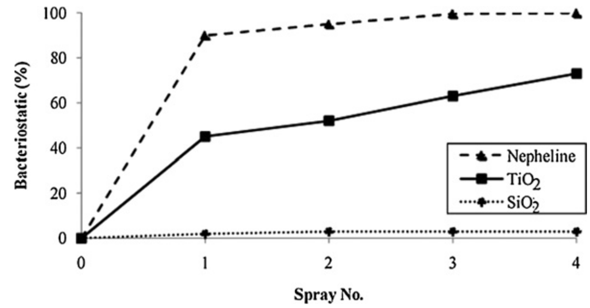

Fig. 7. The bacteriostatic activity of tiles with spray of nepheline, TiO_2, or SiO_2.

4. Conclusions

In this research, a facile and large-scale preparation method for Ag/nepheline antibacterial tiles with the bactericidal activity of 99.9% was presented. We analyzed the antibacterial activity of Ag/nepheline composite in comparison with Ag/TiO_2 and Ag/SiO_2. We reported the higher rates of synthesis and bacteriostatic activity of Ag/nepheline. The results confirmed the hypothesis of uniformity and high antibacterial activity of Ag/nepheline tiles in comparison with other type of samples. It supports the capability of this material for large-scale production in various industrial applications.

Acknowledgement

The authors are grateful to Mr. Toluei, manager of Almas Kavier Tile Co. for sponsoring this research and Mr. Ahmad Movlaei and Mr. Esfandiar Amiri for their helpful guidelines.

References

[1] I. De la Rosa-Gómez, M.T. Olguín, D. Alcántara, Antibacterial behavior of silver-modified clinoptilolite-heulandite rich tuff on coliform microorganisms from wastewater in a column system, Journal of Environment Management 88 (4) (2008) 853–863.
[2] Y. Zhang, F. Chen, J. Zhuang, Y. Tang, D. Wang, Y. Wang, et al., Synthesis of silver nanoparticles via electrochemical reduction on compact zeolite film modified electrodes, Chemical Communications 23 (2002) 2814–2815.
[3] X. Zhao, Q. Zhao, J. Yu, B. Liu, Development of multifunctional photoactive self-cleaning glasses, Journal of Non-Crystalline Solids 354 (12–13) (2008) 1424–1430.
[4] M. Machida, K. Norimoto, T. Kimura, Antibacterial activity of photocatalytic titanium dioxide thin films with photodeposited silver on the surface of sanitary ware, Journal of the American Ceramic Society 88 (1) (2005) 95–100.
[5] L. Yang, L. Lin, S. Weng, Z. Feng, T. Luan, Sexually disrupting effects of nonylphenol and diethylstilbestrol on male silver carp (*Carassius auratus*) in aquatic microcosms, Ecotoxicology and Environmental Safety 71 (2) (2008) 400–411.

[6] J. Chen, C.M. Han, X.W. Lin, Z.J. Tang, S.J. Su, Effect of silver nanoparticle dressing on second degree burn wound, Zhonghua wai ke za zhi (Chinese Journal of Surgery]), 44 (1) (2006) 50–52.
[7] P. Muangman, C. Chuntrasakul, S. Silthram, S. Suvanchote, R. Benjathanung, S. Kittidacha, et al., Comparison of efficacy of 1% silver sulfadiazine and acticoat^{TM} for treatment of partial-thickness burn wounds, Journal of the Medical Association of Thailand 89 (7) (2006) 953–958.
[8] M.S. Cohen, J.M. Stern, A.J. Vanni, R.S. Kelley, E. Baumgart, D. Field, et al., In vitro analysis of a nanocrystalline silver-coated surgical mesh, Surgical Infections 8 (3) (2007) 397–403.
[9] H.Y. Lee, H.K. Park, Y.M. Lee, K. Kim, S.B. Park, A practical procedure for producing silver nanocoated fabric and its antibacterial evaluation for biomedical applications, Chemical Communications 28 (2007) 2959–2961.
[10] N. Vigneshwaran, A.A. Kathe, P.V. Varadarajan, R.P. Nachane, R.H. Balasubramanya, Functional finishing of cotton fabrics using silver nanoparticles, Journal of Nanoscience and Nanotechnology 7 (6) (2007) 1893–1897.
[11] W. Zhang, X. Qiao, J. Chen, Synthesis of silver nanoparticles – effects of concerned parameters in water/oil microemulsion, Materials Science and Engineering B 142 (1) (2007) 1–15.
[12] E.M. Egorova, A.A. Revina, Synthesis of metallic nanoparticles in reverse micelles in the presence of quercetin, Colloids and Surfaces A: Physicochemical and Engineering Aspects 168 (1) (2000) 87–96.
[13] H.-J. Jeon, S.-C. Yi, S.-G. Oh, Preparation and antibacterial effects of Ag–SiO_2 thin films by sol–gel method, Biomaterials 24 (27) (2003) 4921–4928.
[14] A.R. Abbasi, A. Morsali, Syntheses and characterization of AgI nanostructures by ultrasonic method: different morphologies under different conditions, Ultrasonics Sonochemistry 17 (3) (2010) 572–578.
[15] J. Zou, Y. Xu, B. Hou, D. Wu, Y. Sun, Controlled growth of silver nanoparticles in a hydrothermal process, China Particuology 5 (2007) 206–212.
[16] I. Pastoriza-Santos, L.M. Liz-Marzán, Formation of PVP-protected metal nanoparticles in DMF, Langmuir 18 (7) (2002) 2888–2894.
[17] M. Pang, J. Hu, H.C. Zeng, Synthesis, morphological control, and antibacterial properties of hollow/solid Ag_2S/Ag heterodimers, Journal of the American Chemical Society 132 (31) (2010) 10771–10785.
[18] R. Jin, Y. Cao, C.A. Mirkin, K.L. Kelly, G.C. Schatz, J.G. Zheng, Photoinduced conversion of silver nanospheres to nanoprisms, Science 294 (5548) (2001) 1901–1903.
[19] Y. Lai, Y. Chen, H. Zhuang, C. Lin, A facile method for synthesis of Ag/TiO_2 nanostructures, Materials Letters 62 (21–22) (2008) 3688–3690.
[20] X. Li, L. Wang, X. Lu, Preparation of silver-modified TiO_2 via microwave-assisted method and its photocatalytic activity for toluene degradation, Journal of Hazardous Materials 177 (1–3) (2010) 639–647.
[21] X. He, X. Zhao, B. Liu, The synthesis and kinetic growth of anisotropic silver particles loaded on TiO_2 surface by photoelectrochemical reduction method, Applied Surface Science 254 (2008) 1705–1709.
[22] L. Zhang, J.C. Yu, H.Y. Yip, Q. Li, K.W. Kwong, A.-W. Xu, et al., Ambient light reduction strategy to synthesize silver nanoparticles and silver-coated TiO_2 with enhanced photocatalytic and bactericidal activities, Langmuir 19 (24) (2003) 10372–10380.
[23] R.A. Eppler, D.R. Eppler, Glazes and Glass Coatings, The American Ceramic Society, Ohio, 2000.
[24] J. Husheng, H. Wensheng, W. Liqiao, X. Bingshe, L. Xuguang, The structures and antibacterial properties of nano-SiO_2 supported silver/zinc–silver materials, Dental Materials 24 (2) (2008) 244–249.
[25] L. Armelao, D. Barreca, G. Bottaro, A. Gasparotto, S. Gross, C. Maragno, et al., Recent trends on nanocomposites based on Cu, Ag and Au clusters: a closer look, Coordination Chemistry Reviews 250 (11–12) (2006) 1294–1314.
[26] L. Esposito, A. Salem, A. Tucci, A. Gualtieri, S.H. Jazayeri, The use of nepheline-syenite in a body mix for porcelain stoneware tiles, Ceramics International 31 (2) (2005) 233–240.
[27] F. Burat, O. Kangal, G. Onal, An alternative mineral in the glass and ceramic industry: nepheline syenite, Minerals Engineering 19 (4) (2006) 370–371.
[28] R. Bolger, Feldspar and nepheline syenite, Industrial Minerals 332 (1995) 25–45.
[29] C.W. Bale, P. Chartrand, S.A. Degterov, G. Eriksson, K. Hack, R. Ben Mahfoud, et al., FactSage thermochemical software and databases, Calphad - Computer Coupling of Phase Diagrams and Thermochemistry 26 (2) (2002) 189–228.
[30] Q. Li, S. Mahendra, D.Y. Lyon, L. Brunet, M.V. Liga, D. Li, et al., Antimicrobial nanomaterials for water disinfection and microbial control: potential applications and implications, Water Research 42 (18) (2008) 4591–4602.
[31] A.D. Russell, W.B. Hugo, Antimicrobial activity and action of silver, Progress in Medicinal Chemistry 31 (1994) 351–370.
[32] B.S. Atiyeh, M. Costagliola, S.N. Hayek, S.A. Dibo, Effect of silver on burn wound infection control and healing: review of the literature, Burns 33 (2) (2007) 139–148.
[33] M.K. Seery, R. George, P. Floris, S.C. Pillai, Silver doped titanium dioxide nanomaterials for enhanced visible light photocatalysis, Journal of Photochemistry and Photobiology A: Chemistry 189 (2–3) (2007) 258–263.
[34] D. Nelson, P.D. Marcato, G.I.H. De Souza, O.L. Alves, E. Esposito, Antibacterial effect of silver nanoparticles produced by fungal process on textile fabrics and their effluent treatment, Journal of Biomedical Nanotechnology 3 (2007) 203–208.
[35] A.G. Nazari, A. Tahari, F. Moztarzadeh, M. Mozafari, M. Bahrololoom, Ion exchange behaviour of silver-doped apatite micro-and nanoparticles as antibacterial biomaterial, Micro & Nano Letters, IET 6 (8) (2011) 713–717.
[36] M. Dondi, C. Iglesias, E. Dominguez, G. Guarini, M. Raimondo, The effect of kaolin properties on their behaviour in ceramic processing as illustrated by a range of kaolins from the Santa Cruz and Chubut Provinces, Patagonia (Argentina), Applied Clay Science 40 (1–4) (2008) 143–158.
[37] L. Zhang, J.C. Yu, A simple approach to reactivate silver-coated titanium dioxide photocatalyst, Catalysis Communications 6 (10) (2005) 684–687.
[38] W. Zhang, X. Qiao, J. Chen, Synthesis and characterization of silver nanoparticles in AOT microemulsion system, Chemical Physics 330 (2006) 495–500.
[39] P. Knauth, J. Schoonman, Nanostructured Materials – Selected Synthesis Methods, Properties and Applications, Kluwer Academic Publishers, New York/Boston/Dordrecht/London/Moscow, 2004.
[40] L. Suber, I. Sondi, E. Matijević, D.V. Goia, Preparation and the mechanisms of formation of silver particles of different morphologies in homogeneous solutions, Journal of Colloid and Interface Science 288 (2) (2005) 489–495.